Research Article

Fade Li, Xinxin Zhu, Jiyuan Cui, Shuqiang Ding, Mengmeng Yu, and Hongzhen Wang*

Synthesis of migration-resistant antioxidant and its application in natural rubber composites

https://doi.org/10.1515/epoly-2024-0065 received July 02, 2024; accepted September 06, 2024

Abstract: In this article, a novel migration-resistant antioxidant (CGE-g-PPDA) was synthesized using cardanol glycidyl ether (CGE) and p-aminodiphenylamine (PPDA) and characterized by infrared spectroscopy, indicating that the antioxidant has been successfully synthesized. CGE-g-PPDA and other different types of antioxidants were added to natural rubber (NR) to make anti-aging NR composites, which were tested and characterized by processing properties, aging resistance, thermal stability, cross-linking density retention properties, and migration resistance. Comparative results showed that CGE-g-PPDA could reduce the Mooney viscosity of NR, improve its processing performance, prolong the oxidation induction time of materials, give longterm protection to the rubber, and improve the cross-linking retention rate of materials. In addition, the migration resistance and solvent extraction resistance of antioxidant CGEg-PPDA were significantly better than that of antioxidant 4020, with higher stability. CGE-g-PPDA, as a new type of migration-resistant antioxidant, has a potential application value.

Keywords: cardanol glycidyl ether, migration-resistant antioxidant, CGE-g-PPDA, natural rubber composites, aging resistance

Fade Li, Xinxin Zhu, Jiyuan Cui, Mengmeng Yu: Key Laboratory of Rubber-Plastics, Ministry of Education/Shandong Provincial Key Laboratory of Rubber-Plastics, School of Polymer Science and Engineering, Qingdao University of Science and Technology, Qingdao, 266042, China

Shuqiang Ding: Zhongce Rubber (Tianjin) Co., Ltd., Tianjin, 300450,

1 Introduction

Natural rubber (NR), as an indispensable raw material, has high elasticity, strength, and excellent resilience and is widely used in fields such as tires, medical, and aerospace (1–6). NR is mainly composed of *cis*-1,4-polyisoprene (7–11), with a large number of unsaturated double bonds in the molecular chains (12), which has a high degree of unsaturation (13), and due to the presence of side methyl groups, the double bond carbon is more active, in the light, high temperature, and other conditions, and is prone to irreversible aging degradation and cross-linking (14), leading to a decrease in the physical properties of NR products (15). Therefore, the selection of antioxidants is very important during the processing of NR (16).

US Tire Manufacturers Association (USTMA) is seeking a replacement for conventional antioxidant 4020, which produces toxic particles during tire use. PPDA, as a highly effective antioxidant, grafted to NR, can provide long-lasting protection, but due to the low content of isomerization groups in the NR molecular chains, only a small amount of PPDA reacts with the NR molecular chains. To solve this problem, in this article, cardanol glycidyl ether (CGE) was selected to react with PPDA to synthesize a new migration-resistant antioxidant.

CGE contains an unsaturated double bond at one end and a reactive oxygen-containing group at the other end, and its molecular formula is shown in Figure 1, with a relative molecular mass of about 360. During the reaction process, the amino group of PPDA and the epoxy group of CGE underwent epoxidation amination reaction to synthesize CGE-g-PPDA. The synthesized CGE-g-PPDA contains unsaturated double-bonded carbon, which can undergo covulcanization with NR to achieve chemical bonding with the rubber matrix, thus improving the stability and utilization of the antioxidant. Moreover, CGE is derived from biomass cashew nut phenol, which is a natural phenolic compound extracted from cashew nut shell liquid, and is a renewable biomass resource (17–19), so the selection of CGE as the grafting monomer of PPDA can reduce the production cost as well as avoid environmental pollution.

^{*} Corresponding author: Hongzhen Wang, Key Laboratory of Rubber-Plastics, Ministry of Education/Shandong Provincial Key Laboratory of Rubber-Plastics, School of Polymer Science and Engineering, Qingdao University of Science and Technology, Qingdao, 266042, China, e-mail: qustwhz@163.com

Figure 1: Cardanol glycidyl ether.

2 Experimental

2.1 Materials

CGE was produced by Jiangsu Runfeng Synthetic Technology Co. NR latex was produced by Hainan Natural Rubber Industry Group Co. *p*-Aminodiphenylamine (PPDA) was produced by Bailing Wei Technology Co. Carbon black (CB) 330 was produced by Shanghai Cabot Chemical Co. ZnO, stearic acid (SA), sulfur (S), accelerator N-tert-butylbenzothiazole-2-sulphenamide (TBBS), and antioxidant 4020 were commercially available industrial products.

The experimental formula is shown in Table 1.

2.2 Synthesis of migration-resistant antioxidant CGE-g-PPDA

In all, 17.8 g of CGE and 3.7 g of PPDA were added to a three-necked flask, the device was placed in an oil bath at 100°C, stirred until PPDA was completely dissolved in CGE, and

Table 1: Formula of NR compounds (phr)

	NR	4020/NR	CGE + PPDA/NR	CGE-g-PPDA/NR
NR	100	100	100	100
ZnO	5	5	5	5
SA	2	2	2	2
CB 330	35	35	35	35
S	2.25	2.25	2.25	2.25
TBBS	0.7	0.7	0.7	0.7
4020		1.5		
CGE + PPDA			1.5	
CGE-g-PPDA				1.5

then the temperature was raised to 165°C, and after the temperature of the system was stabilized, the reaction was allowed to run for 4 h. CGE-g-PPDA could be obtained, and the reaction product was a dark brown viscous liquid.

The amino active group of PPDA undergoes epoxy amination reaction with the epoxy group of CGE to obtain the reaction product CGE-g-PPDA, which has a –NH group and C=C double bond structure in the molecular chain (Figure 2). The –NH group can capture the macromolecular free radicals generated during the aging of rubber to prevent materials aging. The C=C double bond can undergo co-vulcanization reaction with the rubber, thus improving the migration resistance of the antioxidant.

2.3 Preparation of aging-resistant NR composites

Preparation of composites: Set the initial temperature of the internal mixer (XSM-500, Shanghai Kechuang Rubber & Plastic Machinery Co., Ltd.) at 70°C, the rotation speed at 65 rpm, add NR solid raw rubber, small molecule additives, antioxidant, and CB sequentially, among which CB was added to the internal mixer in two times, the mixing time was 7.5 min, and the rubber was discharged. The discharged rubber and sulfur vulcanization system were added to the open two-roll mill (X (S) K-160, Shanghai Double Wing Rubber & Plastic Machinery Co., Ltd.) for two-stage mixing, the roll pitch was set to 0.2 mm for mill run, and then the roll pitch was set to 2 mm to make rubber film. The produced rubber was placed for 24 h, according to the process optimum cure time t_{90} , the vulcanization temperature was set at 150°C. The materials were named NR, 4020/NR, CGE + PPDA/NR, and CGE-g-PPDA/NR according to the type of antioxidant.

2.4 Characterization

2.4.1 Infrared spectroscopy test

Structural analysis was performed using Fourier transform infrared (FTIR) spectroscopy (VERTEX 70, BRUKER,

$$NH - NH_2 + CH_2 - CH$$

Figure 2: Synthesis of CGE-q-PPDA.

Germany) in total reflection scanning mode with a scanning range of $400-4,000 \text{ cm}^{-1}$.

2.4.2 Mooney viscosity

Mooney viscosity tests were conducted on the mixed rubber according to GB/T 1232.1-2000; two circular rubber films with a diameter of about 50 mm and a mass of 10 g were cut and tested using a Mooney viscometer (MV-2000, the US Alpha Company) for the test, the test temperature was 100°C, preheated for 1 min, and the test time was 4 min.

2.4.3 Tensile property test

Five standard samples of each composite material were made by molds and tested by a Zwick tensile tester (AT-7000S, Zwick Roell, Germany) according to GB/T 528-2009, and the median was taken as the test result.

2.4.4 Oxidation induction time (OIT)

According to the national standard GB/T 19466.6-2009, the OIT of vulcanizates was tested by a differential scanning calorimeter (204 F1, NETZSCH, Germany).

2.4.5 Thermo-oxidative aging property

The thermo-oxidative aging property test was conducted according to the national standard GB/T 3512-2014. The stretching samples were placed in the aging box at 100°C and aged for a certain period of time, taken out and parked for 12 h for mechanical properties and the cross-linking density test, and according to Eq. 1 to calculate the aging coefficient of the vulcanizates (k), the larger the value, the stronger the aging resistance of the material

$$k = \frac{f_{\rm a}}{f_{\rm b}} \tag{1}$$

where f_a is the tensile strength of the material after aging × elongation at break and $f_{\rm u}$ is the tensile strength of the material before aging × elongation at break.

2.4.6 Cross-linking density and its retention rate

The cross-linking density of the composite material was determined by the swelling method, in which about 0.20 g of the vulcanizate was weighed and placed in 20 g of the toluene solution. The sample was removed after 7 days, and the residual toluene on the surface of the vulcanizate was wiped off with a filter paper and weighed, and then the vulcanizate was placed in a 60°C blast drying oven (DHG, Guangzhou Handy Environmental Test Equipment Co., Ltd.) until the weight stopped changing, and then removed for weighing. The cross-linking density $V_{\rm e}$ of the cured rubber was calculated according to Eq. 2. The average of three test results was taken as the final test result

$$V_{\rm e} = -\frac{1}{v} \left[\frac{\ln(1 - V_2) + V_2 + \chi V_2^2}{V_2^{1/3}} \right]$$
 (2)

where V_e represents the cross-linking density of vulcanized rubber, mol·cm⁻³; V_2 represents the volume fraction of the rubber phase in dissolved vulcanized rubber; γ represents the rubber and solvent interaction coefficient, 0.3795; and U represents the molar volume of solvent, $106.4 \text{ cm}^3 \cdot \text{mol}^{-1}$.

The volume fraction V_2 of the rubber phase in the dissolved vulcanized rubber is calculated as follows:

$$V_2 = \frac{V_1}{V_1 + V_{\text{colvent}}} \tag{3}$$

$$V_{\text{solvent}} = \frac{(m_1 - m_2)}{\rho_{\text{solvent}}} \tag{4}$$

$$V_1 = \frac{m_3 \varphi (1 - \alpha)}{\rho} \tag{5}$$

where m_1 is the mass of the sample before drying after swelling, g; m_2 is the mass of the sample after drying after swelling, g; m_3 is the original mass of the sample, g; α is the mass fraction of extract from pure vulcanizate (NR extracted with acetone, $1 - \alpha = 0.9289$); φ is the mass fraction of pure rubber in the sample; ρ is the density of pure vulcanizate ($\rho = 0.958 \,\mathrm{g \cdot cm^{-3}}$); ρ_{solvent} is the density of solvent $(\rho_{\text{solvent}} \text{ for toluene} = 0.867 \text{ g} \cdot \text{cm}^{-3}); V_1 \text{ is the volume of the}$ rubber phase; and V_{solvent} is the volume of solvent in the rubber after swelling.

The cross-linking density retention rate R_C was calculated according to the following equation:

$$R_{\rm C} = \frac{C_{\rm a}}{C_{\rm u}} \times 100\% \tag{6}$$

where $C_{\rm u}$ and $C_{\rm a}$ refer to the cross-linking density of the material before and after aging, respectively.

2.4.7 Scanning electron microscope (SEM)

The vulcanizate samples of different materials were taken, and their surfaces were sprayed gold for 50, 30, and 30 s at a time, using an SEM (ISM-7500F, Japan Electronics Co., Ltd.) to perform a scanning test, and the accelerating voltage of the test was 5 kV. The frosting of the surface of the material was analyzed after aging according to the scanning results.

2.4.8 Migration resistance

The NR with different antioxidants was contacted with the filter paper. The color change of the filter paper reflected the migration resistance of the antioxidants.

2.4.9 Solvent extraction resistance

The vulcanizate samples of the same size and quality from four types of NR were cut and placed in anhydrous ethanol of the same quality, and the color change was observed to determine the solvent extraction resistance of each antioxidant.

2.4.10 Thermogravimetric analysis

In all, 7–8 mg samples were taken from four types of NR and tested using a thermogravimetric analyzer (209 F1, NETZSCH, Germany); the test environment was oxygen and air atmosphere, respectively, with a set rate of temperature increase of 10°C·min⁻¹, and a temperature range of room temperature ~700°C.

3 Results and discussion

3.1 Structural characterization of CGEg-PPDA

Figure 3 shows the FTIR spectrum of PPDA, CGE, and the reaction product CGE-g-PPDA. In the infrared spectrum of PPDA, the broad absorption peaks appearing around 3,440 cm⁻¹ are attributed to the N–H stretching vibration absorption peaks, the absorption peaks at 2,910 cm⁻¹ are attributed to the C–H stretching vibration, and 1,495 and 1,517 cm⁻¹ are attributed to the vibration absorption peaks of the mono-substituted benzene ring and the bis-substituted benzene ring. In the IR spectrum of CGE, 2,925 and 2,851 cm⁻¹ are the stretching vibration peaks of the methylene group, and the characteristic absorption peaks of the epoxy group appear at 915 and 862 cm⁻¹. In the infrared spectrum of the compounds, the characteristic peaks of the

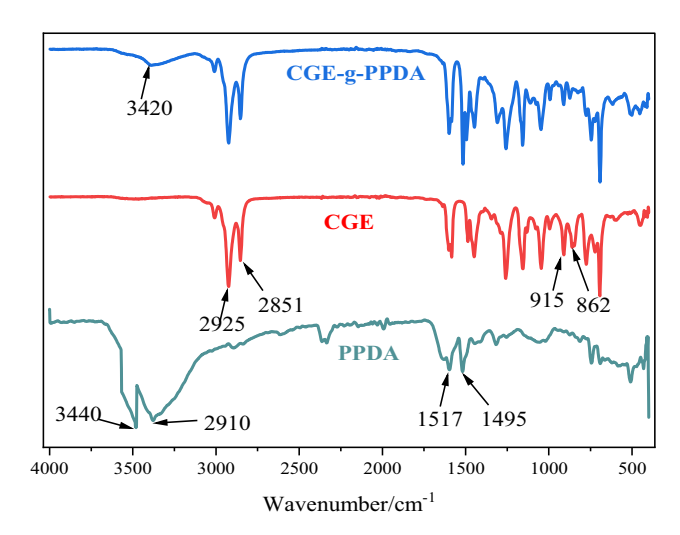


Figure 3: FTIR spectrum of PPDA CGE and the product.

amino group at 3,440 cm⁻¹ and the epoxy group at 915 cm⁻¹ basically disappear, and a new absorption peak appears at 3,420 cm⁻¹, which can be analyzed as the vibrational absorption peaks of –OH generated by ring opening of an epoxy group, so it can be inferred that the PPDA reacts with the CGE, and the target product, CGE-g-PPDA, is successfully synthesized.

3.2 Effect of antioxidants on the Mooney viscosity of NR compounds

Figure 4 shows the Mooney viscosity of NR materials after the addition of various antioxidants. From the figure, it can be seen that the Mooney viscosity of the NR material without the addition of antioxidant is 29.8, and the Mooney

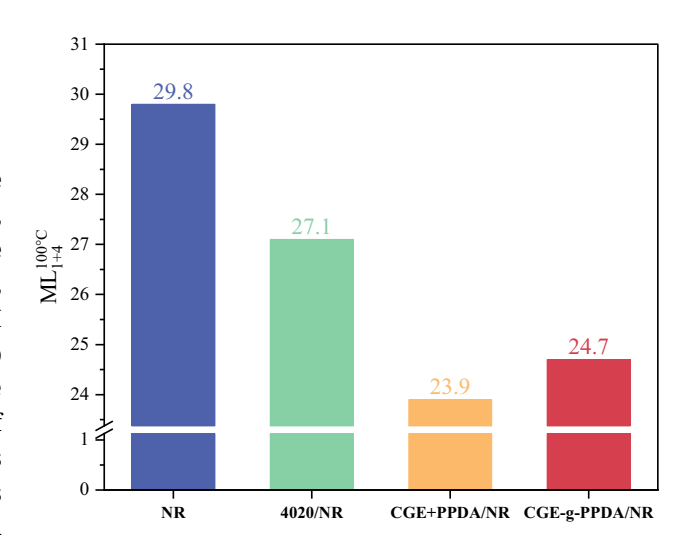


Figure 4: Mooney viscosity of NR compounds.

viscosity of the material after the addition of different antioxidants is reduced to different degrees. The Mooney viscosity of 4020/NR is reduced by 2.7 units; this is because the antioxidant molecules are distributed between the molecular chains of the rubber, increasing the spacing between the molecular chains, and the antioxidant 4020 has a certain shearing effect on the molecular chains of the rubber during processing, resulting in the Mooney viscosity of 4020/NR being lower than the Mooney viscosity of NR. The Mooney viscosity of CGE + PPDA/NR is reduced by 5.9 units, and the Mooney viscosity of CGE-g-PPDA/NR is reduced by 5.1 units. CGE is an oily substance with a strong plasticizing effect, so the reduction in Mooney viscosity of NR with CGE is greater than that of NR with 4020. Comparing the Mooney viscosity of CGE + PPDA/NR and CGE-g-PPDA/NR, the reason is that after the addition of CGE and PPDA blends, CGE and PPDA do not react, and CGE is more free to penetrate into the rubber material, which has a plasticizing effect on NR, and therefore, the Mooney viscosity of CGE + PPDA/NR is lower than that of CGE-g-PPDA/NR.

3.3 Effect of antioxidants on the OIT of NR composites

Figure 5 shows the OIT test curves and corresponding OIT values of NR composites containing different antioxidants at 190°C.

The OIT of a material can be used to characterize the strength of the material's resistance to thermo-oxidative

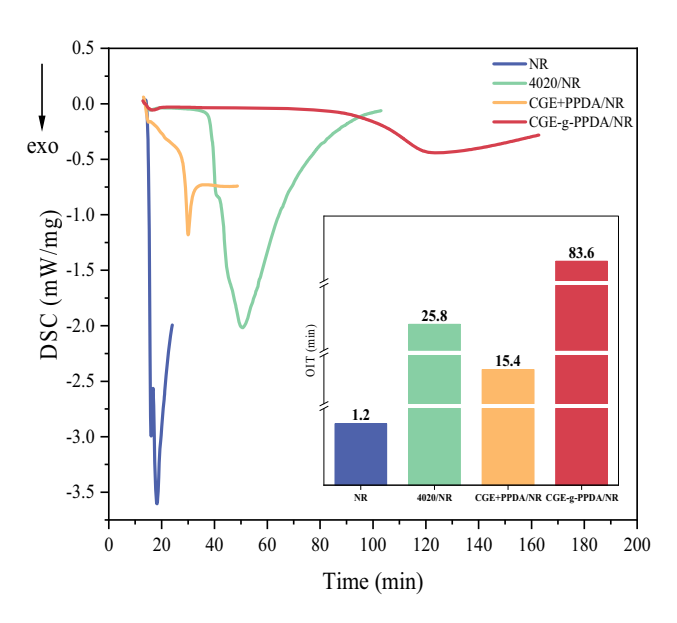


Figure 5: OIT curves of NR compounds.

aging; the longer the OIT, the better the material's resistance to thermo-oxidative aging (20–22).

As can be seen from the test curves in the figure, the curve of the NR composites without antioxidant shows a steep exothermic peak just after the passage of oxygen, and its OIT is the shortest, which is 1.2 min, indicating that the oxidation reaction of the material is the most violent. After the addition of the antioxidants, the oxidation exothermic peaks of the composites tend to level off, and the OIT are significantly prolonged, indicating that all three antioxidants can prolong the OIT of the NR composites. Among them, the OIT of 4020/NR vulcanizate is 25.8 min, the OIT of CGE + PPDA/NR vulcanizate is 15.4 min, and the OIT of CGEg-PPDA/NR vulcanizate is up to 83.6 min, which is three times longer than that of 4020/NR vulcanizate, and the oxidative exothermic peaks of the curves are smooth and gentle, indicating that CGE-g-PPDA can give NR composites a better OIT. The reason is that both 4020 and PPDA contain -NH groups that can trap and passivate oxygen radicals, and all three antioxidants can improve the thermo-oxidative aging resistance of rubber composites. The higher molecular weight of CGE-g-PPDA means that it is less likely to be lost in the rubber matrix through volatilization and migration, and therefore, CGE-g-PPDA/NR has a longer OIT.

3.4 Effect of antioxidants on the thermooxidative degradation behavior of NR composites

Thermogravimetric analysis test curves characterize the thermal stability of the materials and thus evaluate the protective effect of each antioxidant. Figure 6 shows the thermogravimetric curves and specific data for each composite under nitrogen and air atmospheres, respectively.

3.4.1 N₂ atmosphere

The thermogravimetric curves of each NR composite under a nitrogen atmosphere are shown in Figure 6, and the corresponding thermogravimetric characteristic temperatures are given in Table 2.

In the experimental formulation, each component of the rubber is the same except for the type of antioxidant, so the thermal stability of each type of antioxidant can be preliminarily assessed by comparing the temperatures of T_5 %. As can be seen from the table, the temperatures of T_5 % of the four composites, from high to low, are as follows: NR > CGE-g-PPDA/NR > CGE + PPDA/NR > 4020/NR.

6 — Fade Li et al. DE GRUYTER

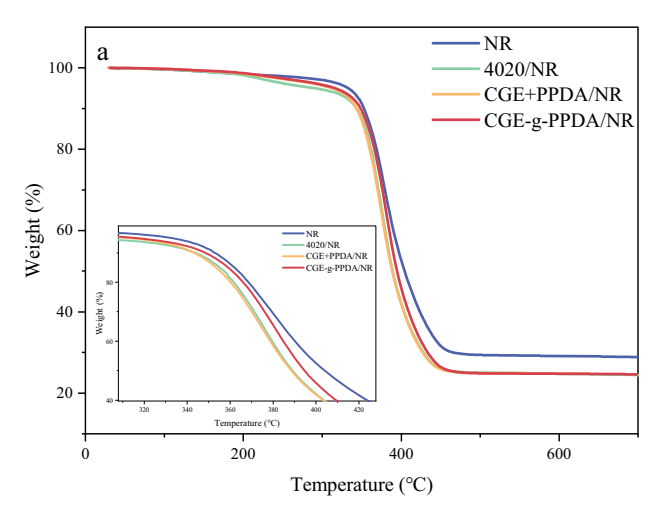


Figure 6: TG (a) and DTG (b) curves of NR compounds in N₂.

 T_{5%} (°C)
 T_{10%} (°C)
 T_{50%} (°C)
 T_{max} (°C)

 NR
 332
 353
 403
 379

 4020/NR
 288
 343
 388
 377

343

347

388

394

375

381

Table 2: TG characteristic temperature of NR compounds in N₂

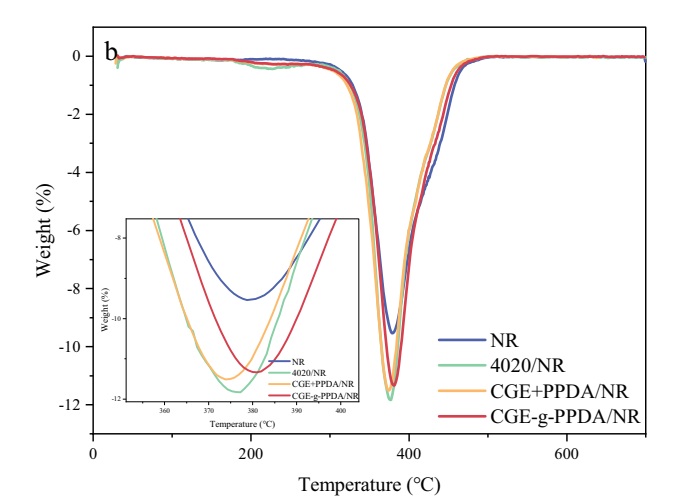
312

325

CGE + PPDA/NR

CGE-q-PPDA/NR

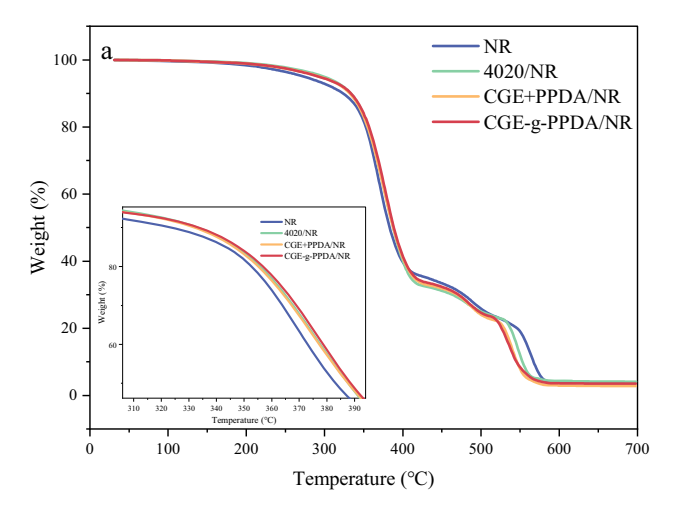
This is because in a nitrogen atmosphere, rubber cannot undergo oxidative degradation due to the absence of oxygen. After adding antioxidants, under the initial temperature rise, antioxidant 4020 is the first to decompose, the antioxidants in PPDA + CGE/NR decompose at a higher temperature, and the antioxidants in CGE-g-PPDA/NR decompose at a higher temperature than PPDA + CGE/NR because of co-vulcanization with NR, which results in the highest $T_5\%$ of NR without antioxidant addition. The $T_5\%$ of the CGE-g-PPDA/NR vulcanizate is 325°C, which is higher



than that of the 4020/NR vulcanizate by 37°C, indicating that the thermal stability of the new antioxidant is much better than that of the traditional antioxidant 4020. Comparing the $T_{\rm max}$ of the two composites, the $T_{\rm max}$ of the CGE-g-PPDA/NR composite is 381°C, the $T_{\rm max}$ of the 4020/NR composite is 377°C, and the $T_{\rm max}$ of the CGE + PPDA/NR composite is 375°C. The former is still higher than the latter two, indicating that the combination of the new antioxidant and rubber is stronger than that of the blends of CGE + PPDA and rubber. The stability of the new migration-resistant antioxidant is higher.

3.4.2 Air atmosphere

The thermogravimetric curves of NR composites under the air atmosphere are shown in Figure 7, and the corresponding thermogravimetric characteristic temperatures





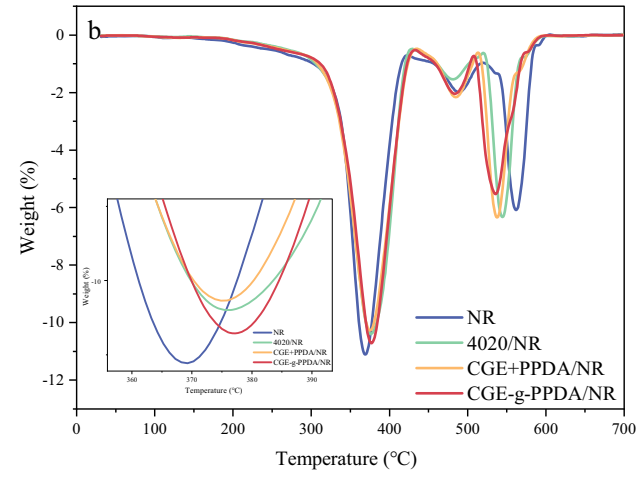


Table 3: TG characteristic temperature of NR compounds in air

	7 _{5%} (°C)	T _{10%} (°C)	7 _{50%} (°C)	T _{max} (°C)
NR	273	323	382	368
4020/NR	298	333	387	376
CGE + PPDA/NR	293	332	387	376
CGE-g-PPDA/NR	293	333	388	377

are shown in Table 3. From the specific data in the table, it can be seen that the $T_5\%$ of 4020/NR composites are 298°C, which is higher than those of the other three composites, and this is because 4020 has a higher migration rate than other antioxidants and can migrate to the surface of the matrix faster and accumulate under the same conditions, which can improve the thermo-oxidative aging property of rubber materials in a short time. Comparing the $T_{\rm max}$ of the four composites, the trend of CGE-g-PPDA/NR > CGE + PPDA/NR = 4020/NR > NR is shown, which indicates that after a period of volatilization and oxidation, the thermo-oxidative aging resistance of CGE-g-PPDA/NR is the most excellent, which is attributed to the more excellent migration resistance of CGE-g-PPDA.

3.5 Effect of antioxidants on the thermooxidative aging properties of NR composites

Table 4 shows the tensile strength, elongation at break, and aging coefficient parameters of the composites before and

after aging. Figure 8 shows the changes in tensile strength, elongation at break, and aging coefficient of the composites at different aging times. From the table, it can be seen that the performance of the four NR composites decreases to different degrees with the aging time, but the CGE-g-PPDA/NR always maintains the best elongation at break and excellent tensile strength at each aging stage, indicating that the aging resistance of the new antioxidant is quite good.

The aging coefficient can be used to characterize the aging resistance of the composites, and the closer the aging coefficient is to 1, the smaller the decrease in the performance of the material compared to that before aging, and the better the effect of the antioxidant. From Figure 8(c), it is easy to see that the aging coefficient of antioxidant 4020 is larger than that of the new antioxidant in 72 h before aging, and with the extension of the aging time, the aging coefficient of 4020/NR starts to be smaller than that of CGEg-PPDA/NR, and the aging coefficient of CGE-g-PPDA is 0.13 in 120 h, which is much higher than the aging coefficient of 4020/NR (0.08). This shows that the anti-aging effect of 4020 is slightly better than that of CGE-g-PPDA in the early stage of aging, while the stability of CGE-g-PPDA is higher, which makes its anti-aging effect better than that of 4020 in the late stage of aging. The reason is that in the early stage of aging, the thermo-oxidative aging resistance of the rubber largely depends on the concentration of antioxidant in the surface layer of the rubber. The molecular weight of 4020 antioxidant is smaller, its movement rate is faster, and it can very easily migrate to the surface of the vulcanizate and accumulate, so the 4020/NR vulcanizate has excellent

Table 4: Mechanical properties before and after aging of NR compounds

		NR	4020/NR	CGE + PPDA/NR	CGE-g-PPDA/NR
100°C × 0 h	Tensile strength (MPa)	22.6	21.6	21.5	22.3
	Elongation at break (%)	626.4	642.1	677.2	738.0
	Aging coefficient	1	1	1	1
100°C × 24 h	Tensile strength (MPa)	17.3	20.8	17.7	19.9
	Elongation at break (%)	512.8	585.5	599.6	621.0
	Aging coefficient	0.63	0.88	0.73	0.75
100°C × 48 h	Tensile strength (MPa)	16.5	17.7	14.2	19.2
	Elongation at break (%)	458.4	489.8	520.9	535.4
	Aging coefficient	0.53	0.63	0.51	0.62
100°C × 72 h	Tensile strength (MPa)	7.9	13.7	10.4	14.2
	Elongation at break (%)	372.1	464.3	448.7	482.1
	Aging coefficient	0.21	0.46	0.32	0.42
100°C × 96 h	Tensile strength (MPa)	4.9	7.6	6.3	9.5
	Elongation at break (%)	281.4	315.5	330.4	350.0
	Aging coefficient	0.10	0.17	0.14	0.20
100°C × 120 h	Tensile strength (MPa)	3.5	4.8	4.0	6.6
	Elongation at break (%)	205.3	225.7	181.2	315.2
	Aging coefficient	0.05	0.08	0.05	0.13

resistance to thermo-oxidative aging. The molecular weight of CGE-g-PPDA is higher than that of 4020, the migration rate is lower, and it has not migrated to the surface in a short time, so the early protective effect of CGE-g-PPDA is not as good as that of small molecule antioxidant 4020, but with the aging time, its antioxidant effect is better than that of 4020. Therefore, as the aging time increases, the content of 4020 in 4020/NR vulcanizate decreases drastically due to continuous migration, and the thermo-oxidative aging resistance of the rubber deteriorates, but CGE-g-PPDA still remains in the rubber matrix, and there are still a large number of free radicals that can be trapped by the -NH group in the CGE-g-PPDA/NR composite, which interrupts chains oxidation and slows down the oxidation rate of the rubber. This proves that the antioxidant CGE-g-PPDA has a higher migration resistance and is more valuable than the traditional antioxidant 4020 in long-term aging environments.

3.6 Effect of antioxidants on cross-linking density retention of NR composites

Table 5 shows the cross-linking density parameters of the four materials at different aging times. Figure 9 shows the change in cross-linking density of the materials and the rate of change in cross-linking density during aging for 120 h. From Table 5 and Figure 9(a), it can be seen that the cross-linking density of the four materials shows a trend of increasing and then decreasing. The reason is that in the pre-aging period, the materials still contain some S, and under the effect of high temperature, further cross-linking of molecular chains will occur, and the cross-linking density will be increased, while in the late aging period, the breakage of molecular chains is dominant. However, it is not difficult to see from the data that the cross-linking density of CGE-g-PPDA/NR composites still

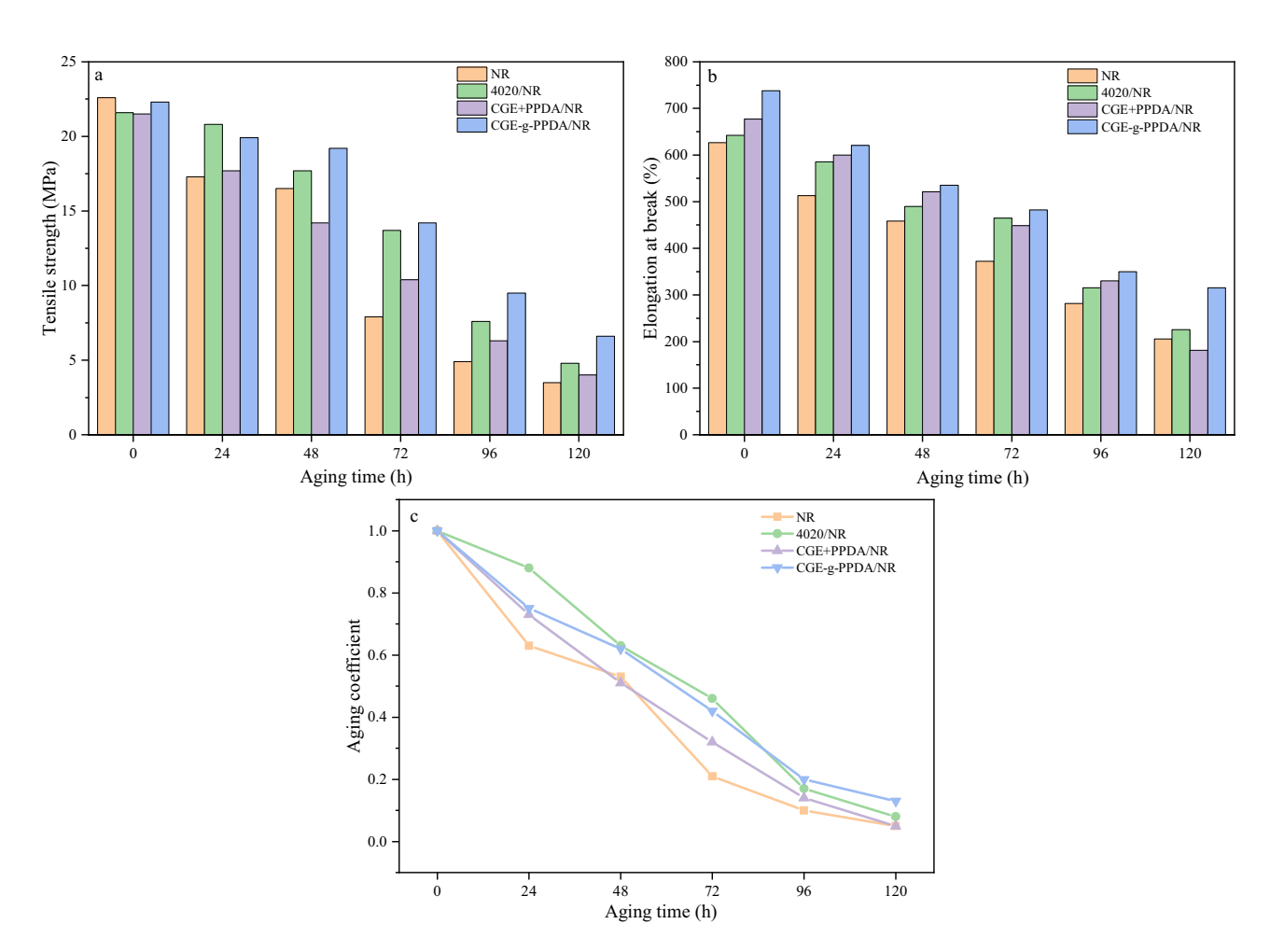


Figure 8: Tensile strength (a), elongation at break (b) before and after aging, and aging coefficient (c) of NR compounds.

Table 5: Cross-linking density of NR compounds (10⁻⁴ mol·cm⁻³)

	Aging time (h)					
	0	24	48	72	96	120
NR	1.416	1.487	1.361	1.321	1.256	1.103
4020/NR	1.700	1.900	1.658	1.610	1.530	1.420
CGE + PPDA/NR	1.523	1.765	1.499	1.241	1.167	1.010
CGE-g-PPDA/NR	1.642	1.848	1.732	1.698	1.592	1.502

remains at a higher level in the late aging period, indicating that its anti-aging properties are excellent.

The cross-linking density retention rate of rubber reflects the ability of the material to resist thermo-oxidative aging, the higher the retention rate, the higher the ability of the rubber to resist thermo-oxidative aging. As shown in Figure 9(b), the cross-linking density change rates of pure NR are all higher than those of rubber composites containing antioxidants, indicating that all three antioxidants can slow down the thermo-oxidative aging of rubber chains. Among them, the CGE-g-PPDA/NR composite has the highest cross-linking density retention rate, indicating that the antioxidant CGE-g-PPDA has better thermo-oxidative aging resistance than the antioxidant 4020.

3.7 Migration resistance of antioxidants

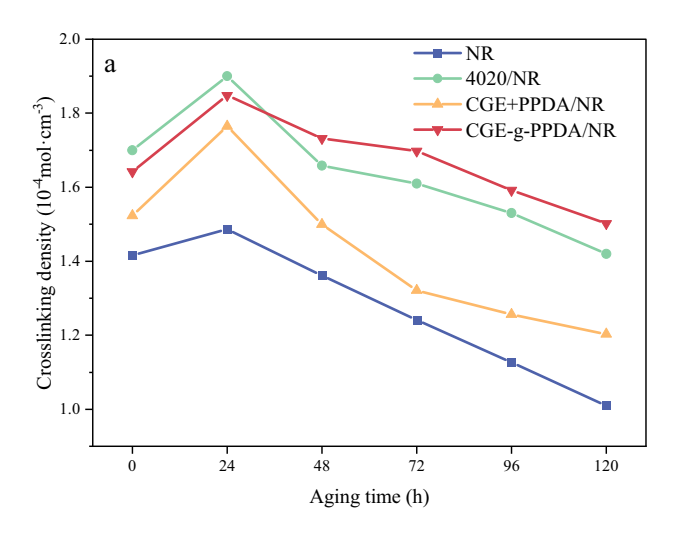
3.7.1 Surface blooming phenomenon

Figure 10 shows the electron micrographs of the surface of the samples after aging the four composites for 120 h. From

the figure, it can be seen that the surface of NR without the addition of antioxidants is very smooth without too much small material exuding. The surface of the NR with 4020 added shows a lot of impurities, resulting in an obvious blooming phenomenon. The NR with CGE + PPDA shows more impurities and a higher degree of blooming. Comparatively, the NR with CGE-g-PPDA has only a small number of impurities on the surface, and the blooming phenomenon is not very obvious, leading to the judgment that CGE-g-PPDA has better migration resistance. This is because 4020, as a small molecule antioxidant, is more likely to migrate to the surface of NR, resulting in the occurrence of a blooming phenomenon. The molecular weight of CGE + PPDA is large, and only a part will migrate to the surface of NR, while CGE-g-PPDA will undergo co-vulcanization with NR, which increases the combination of antioxidant and rubber, so the blooming phenomenon is the least obvious.

3.7.2 Filter paper contamination phenomenon

Figure 11 shows the migration of the four composites on the filter paper. As can be seen from the figure, the NR with no added antioxidant leaves almost no traces on the filter paper. The NR with the addition of antioxidant 4020 leaves extremely clear traces on the filter paper, indicating that the antioxidant 4020 is less resistant to migration. The NR with CGE + PPDA blends leaves a shallow trace on the filter paper, and the antioxidant migrates to some extent. The NR with the addition of the antioxidant CGE-g-PPDA leaves almost no trace on the filter paper, indicating that the antioxidant has excellent migration resistance. This is because the antioxidants in 4020/NR and CGE + PPDA/NR



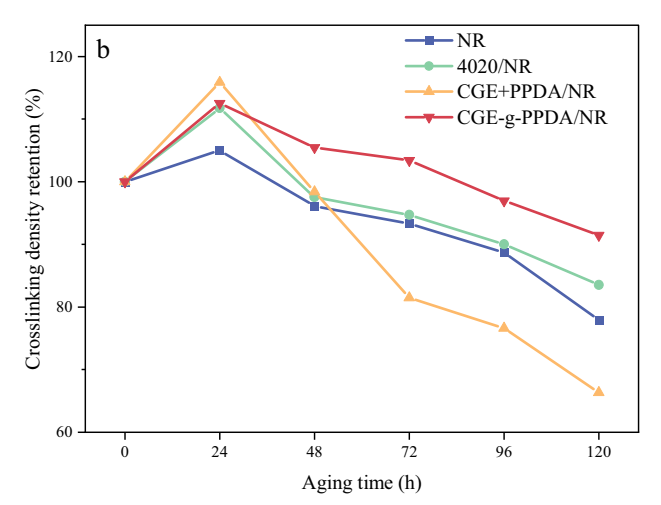


Figure 9: Cross-linking density (a) and retention of cross-linking density (b) of NR compounds.

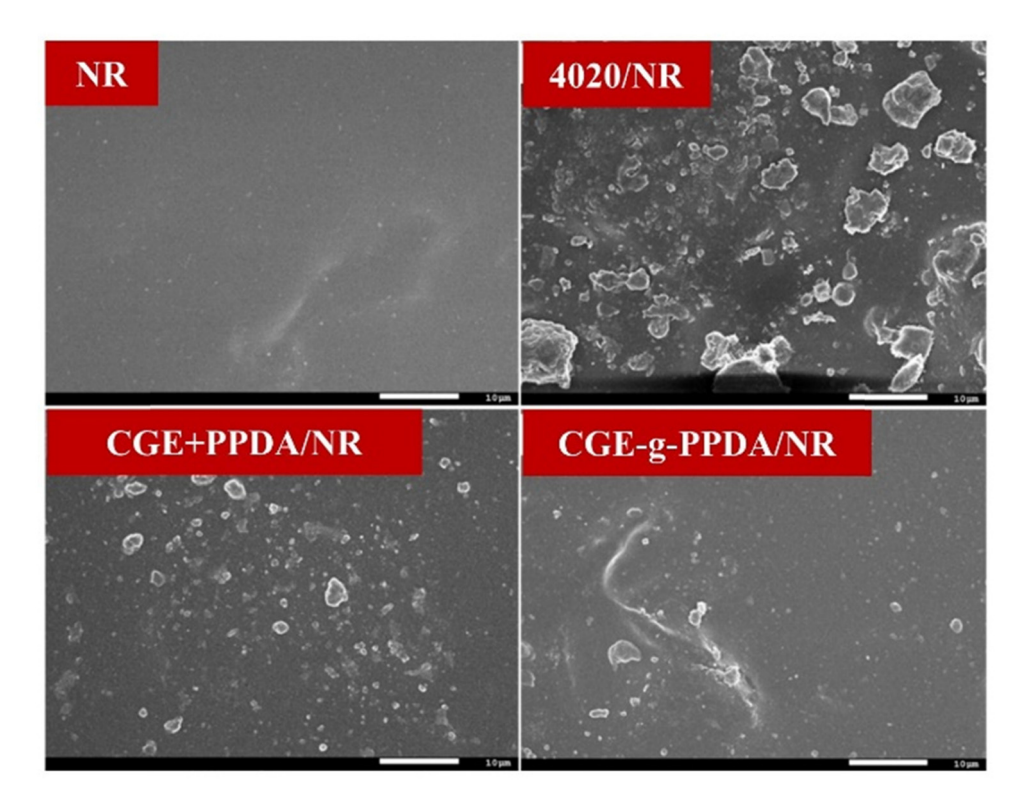


Figure 10: SEM images of NR compounds.

do not undergo co-vulcanization with NR, the antioxidants migrate to the surface of the rubber and contaminate the filter paper. The antioxidants in CGE-g-PPDA/NR can undergo co-vulcanization with NR and are more distributed in the interior of the rubber so that the contamination of the filter paper is small.

3.7.3 Solvent extraction phenomenon

Figure 12 shows the phenomenon of the four composites soaked in anhydrous ethanol for 120 h. Anhydrous ethanol

is a colorless liquid when not soaked. From the figure, it can be seen that there is no change in the anhydrous ethanol in the bottles of the blank control group without the addition of antioxidant; the anhydrous ethanol in the bottles of the NR with the addition of antioxidant 4020 changes to a darker yellow color. The color of the anhydrous ethanol in the bottles of NR with the addition of CGE + PPDA changes to a lighter yellow color, and the color of the anhydrous ethanol in the bottles of NR with the addition of CGE-g-PPDA remains unchanged. This phenomenon indicates that the antioxidant 4020 is the most easily extracted, and the synthetic CGE-g-PPDA is more resistant

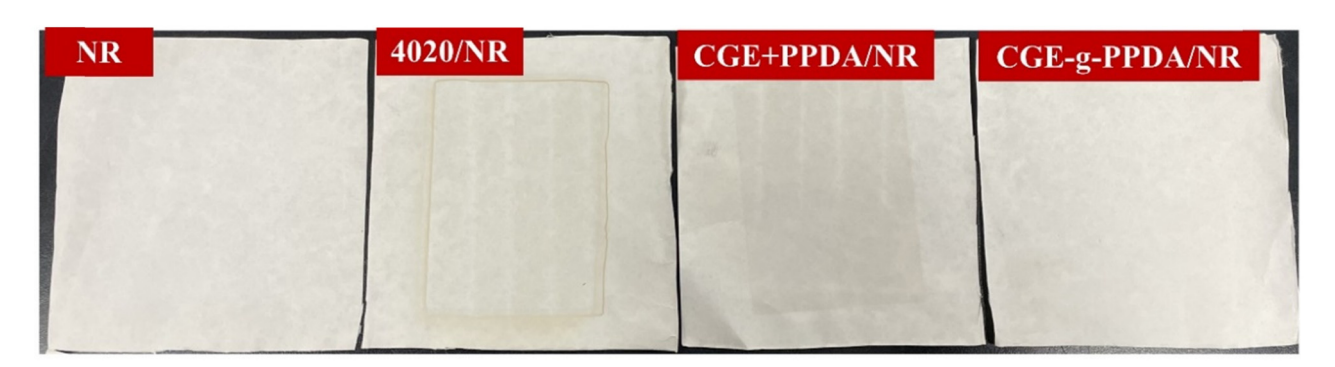


Figure 11: Changes of NR vulcanizates on filter paper.

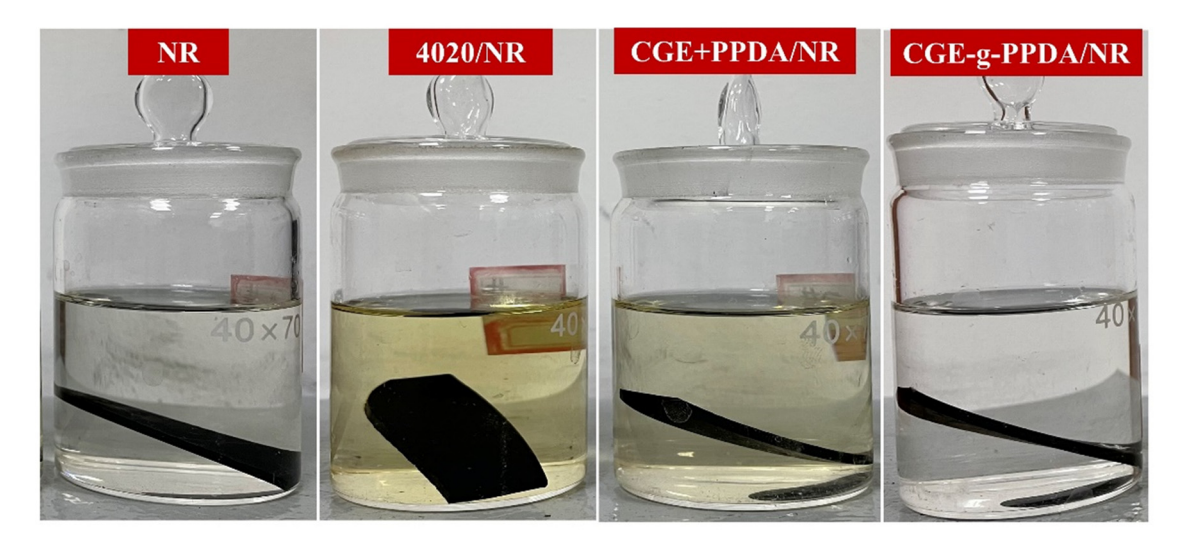


Figure 12: NR vulcanizates soaked in anhydrous ethanol for 120 h.

to solvent extraction. The first reason is that the molecular weight of CGE-g-PPDA is larger than that of antioxidant 4020, and the movement rate is slower. The second reason is that CGE-g-PPDA contains carbon—carbon double bonds, which undergo co-vulcanization reaction with rubber molecular chains during vulcanization. The combination of CGE-g-PPDA and the rubber matrix is tighter and therefore more difficult to extract.

4 Conclusions

In summary, this article first characterizes the structure of the synthesized product through FTIR, indicating the success of the new antioxidant CGE-g-PPDA. Then, CGE-g-PPDA is applied to NR, and the test shows that the antioxidant CGE-g-PPDA can significantly reduce the Mooney viscosity of NR and improve the processing performance of NR. Second, in the OIT test results, the OIT of 4020/NR is only 25.8 min, while that of CGE-g-PPDA is as long as 83.6 min, which proves that CGE-g-PPDA can effectively improve the thermal stability of NR. Tests on the tensile properties and cross-linking density of the materials before and after aging show that CGE-g-PPDA can improve the aging resistance and cross-linking density retention of NR. Finally, through the filter paper simulation experiment and solvent extraction experiment, it can be seen that the migration resistance and solvent extraction resistance of the antioxidant CGE-g-PPDA are obviously better than that of the traditional small molecule antioxidant 4020. Therefore, CGE-g-PPDA can endow NR with excellent thermo-oxidative aging resistance and longterm protection and has broad application prospects.

Funding information: This work was supported by the National Key Research and Development Program of China (No.2022YFD2301204).

Author contributions: Fade Li: writing-original draft, writing-review & editing, formal analysis; Xinxin Zhu: writing-original draft, visualization, data curation; Jiyuan Cui: data curation, investigation; Shuqiang Ding: resources, investigation; Mengmeng Yu: investigation; data curation; Hongzhen Wang: investigation, resources, supervision, project administration. All authors have read and agreed to the published version of the manuscript.

Conflict of interest: Authors state no conflict of interest.

Data availability statement: All relevant data are provided within this article.

References

- (1) Seentrakoon B, Junhasavasdikul B, Chavasiri W. Enhanced UV-protection and antibacterial properties of natural rubber/rutile-TiO₂ nanocomposites. Polym Degrad Stab. 2013;98(2):566–78. doi: 10.1016/j.polymdegradstab.2012.11.018.
- (2) Ibrahim S, Othman N, Sreekantan S, Tan KS, Mohd Nor Z, Ismail H. Preparation and characterization of low-molecular-weight natural rubber latex via photodegradation catalyzed by nano TiO₂. Polymers. 2018;10(11):1216. doi: 10.3390/polym10111216.
- (3) Mohapatra S, Alex R, Nando GB. Cardanol grafted natural rubber: a green substitute to natural rubber for enhancing silica filler dispersion. J Appl Polym Sci. 2016;133(8):43057. doi: 10.1002/app.43057.
- (4) Yantaboot K, Amornsakchai T. Effect of mastication time on the low strain properties of short pineapple leaf fiber reinforced natural

- (5) Chen L, Yu G, Zhuang T, Pang X. Reinforcing effects of carbon nanotubes on graphene/trans-1,4-polyisoprene/natural rubber composites. J Polym Res. 2022;29(9):387. doi: 10.1007/s10965-022-03231-y.
- (6) Saengthaveep S, Magaraphan R. Natural rubber–toughened nylon12 compatibilized by polystyrene/natural rubber blend. Adv Polym Technol. 2013;32(3):21352. doi: 10.1002/adv.21352.
- (7) Spratte T, Plagge J, Wunde M, Klüppel M. Investigation of straininduced crystallization of carbon black and silica filled natural rubber composites based on mechanical and temperature measurements. Polymer. 2017;115:12–20. doi: 10.1016/j.polymer.2017.03.019.
- (8) Borges FA, de Barros NR, Garms BC, Miranda MCR, Gemeinder JLP, Ribeiro-Paes JT, et al. Application of natural rubber latex as scaffold for osteoblast to guided bone regeneration. J Appl Polym Sci. 2017;134(39):45321. doi: 10.1002/app.45321.
- (9) Chandran V, Raj TM, Lakshmanan T. Effect of recycled rubber particles and silica on tensile and tear properties of natural rubber composites. Mater Sci. 2016;22(2):256–61. doi: 10.5755/j01.ms.22. 2.7330.
- (10) Wang M, Wang R, Chen X, Kong Y, Huang Y, Lv Y, et al. Effect of nonrubber components on the crosslinking structure and thermooxidative degradation of natural rubber. Polym Degrad Stab. 2022;196:109845. doi: 10.1016/j.polymdegradstab.2022.109845.
- (11) Ibrahim S, Othman N, Yusof NH. Preparation, characterization and properties of liquid natural rubber with low non-rubber content via photodegradation. Polym Bull. 2021;78:559–75. doi: 10.1007/ s00289-019-03030-4.
- (12) Naebpetch W, Thumrat S, Indriasari, Nakaramontri Y, Sattayanurak S. Effect of glycerol as processing oil in natural rubber/carbon black composites: Processing, mechanical, and thermal aging properties. Polymers. 2023;15(17):3599. doi: 10.3390/ polym15173599.
- (13) Hinchiranan N, Lertweerasirikun W, Poonsawad W, Rempel GL, Prasassarakich P. Hydrogenated natural rubber blends: Aspect on thermal stability and oxidative behavior. J Appl Polym Sci. 2009;113(3):1566–75. doi: 10.1002/app.30034.

- (14) Shuhaimi NHH, Ishak NS, Othman N, Ismail H, Sasidharan S. Effect of different types of vulcanization systems on the mechanical properties of natural rubber vulcanizates in the presence of oil palm leaves-based antioxidant. J Elastomers Plast. 2014;46(8):747–64. doi: 10.1177/0095244313489910.
- (15) Zhou MZ, Wang HR, Guo X, Wei YC, Liao S. Synergistic effect of thermal oxygen and UV aging on natural rubber. e-Polymers. 2023;23(1):20230016. doi: 10.1515/epoly-2023-0016.
- (16) Zhong B, Lin J, Liu M, Jia Z, Luo Y, Jia D, et al. Preparation of halloysite nanotubes loaded antioxidant and its antioxidative behaviour in natural rubber. Polym Degrad Stab. 2017;141:19–25. doi: 10.1016/j.polymdegradstab.2017.05.009.
- (17) Maia FJN, Ribeiro VGP, Lomonaco D, Luna FMT, Mazzetto SE. Synthesis of a new thiophosphorylated compound derived from cashew nut shell liquid and study of its antioxidant activity. Ind Crop Prod. 2012;36(1):271–5. doi: 10.1016/j.indcrop.2011.10.019.
- (18) Mohapatra S, Nando GB. Cardanol: A green substitute for aromatic oil as a plasticizer in natural rubber. RSC Adv. 2014;4(30):15406–18. doi: 10.1039/c3ra46061d.
- (19) Mongkhoun E, Charmi G, Grier-Boisgontier J, Niang F, Gomes M, Quienne B, et al. Ring-opening (co) polymerization of cardanol glycidyl ether. Polym Adv Technol. 2024;35(2):e6320. doi: 10.1002/ pat.6320.
- (20) Bu J, Huang X, Li S, Jiang P. Significantly enhancing the thermal oxidative stability while remaining the excellent electrical insulating property of low density polyethylene by addition of antioxidant functionalized graphene oxide. Carbon. 2016;106:218–27. doi: 10.1016/j.carbon.2016.05.020.
- (21) Balzadeh Z, Arabi H. Novel phenolic antioxidant-functionalized dendritic polyethylene: Synthesis by tailor-made nickel (II) αdiimine-catalyzed copolymerization and its characteristics as nonreleasing additive. React Funct Polym. 2017;111:68–78. doi: 10.1016/ i.reactfunctpolym.2016.11.005.
- (22) Wei H, Zhou J, Zheng J, Huang G. Antioxidation efficiency and reinforcement performance of precipitated-silica-based immobile antioxidants obtained by a sol method in natural rubber composites. RSC Adv. 2015;5(112):92344–53. doi: 10.1039/ c5ra15435a.